

Orbital-order melting in rare-earth manganites: the role of super-exchange

Andreas Flesch,¹ Guoren Zhang,¹ Erik Koch,² and Eva Pavarini^{1,*}

¹ *Institute for Advanced Simulation and JARA, Forschungszentrum Jülich, 52425 Jülich, Germany*

² *German Research School for Simulation Sciences, 52425 Jülich, Germany*

We study the mechanism of orbital-order melting observed at temperature T_{OO} in the series of rare-earth manganites. We find that many-body super-exchange yields a transition-temperature T_{KK} that decreases with decreasing rare-earth radius, and increases with pressure, opposite to the experimental T_{OO} . We show that the tetragonal crystal-field splitting reduces T_{KK} further increasing the discrepancies with experiments. This proves that super-exchange effects, although very efficient, in the light of the experimentally observed trends, play a minor role for the melting of orbital ordering in rare-earth manganites.

PACS numbers: 71.27.+a, 75.25.Dk, 71.30.+h, 71.28.+d, 71.10.Fd

The role of orbital degrees of freedom [1] in the physics of LaMnO_3 , and in particular the co-operative Jahn-Teller transition, has been debated since long [1–5]. Ab-initio LDA+ U calculations show that Coulomb repulsion effects are key to understanding the orbitally-ordered antiferro-magnetic ground state [4]. Super-exchange alone, however, is not sufficient [6] to explain the presence of co-operative Jahn-Teller distortions in nanoclusters up to $T \sim 1150$ K [7, 8] (orbitally disordered phase). Still, superexchange effects are rather large: T_{KK} , the temperature at which superexchange alone would drive the transition, is remarkably close to T_{OO} , the temperature at which the *co-operative* Jahn-Teller distortion disappears in resonant X-ray and neutron scattering [9]. This fact could indicate that super-exchange, although insufficient to explain the persistence of Jahn-Teller distortions in the orbitally disordered phase, plays a major role in the orbital order-to-disorder transition (orbital order melting) observed at T_{OO} . Here we resolve this issue.

Remarkably, orbital-order melting has been observed [10–12] in the full series of orthorhombic rare-earth (RE) manganites REMnO_3 . These systems are perovskites (Fig. 1) with electronic configuration $\text{Mn } 3d^4 (t_{2g}^3 e_g^1)$. In the co-operative Jahn-Teller phase ($T < T_{OO}$), the MnO_6 octahedra are tilted and rotated, and exhibit a sizable Jahn-Teller distortion with long and short MnO bonds antiferro-ordered in the xy plane, and ferro-ordered along z (Fig. 1). Neutron and X-ray diffraction data show that T_{OO} increases from 750 K to ~ 1500 K with decreasing ionic radius IR ($\text{La} \rightarrow \text{Dy}$) [9–12]; under increasing pressure eventually orbital order melts [13, 14], while JT distortions still persist in nanoclusters [8].

The strength of super-exchange is directly linked to the amplitude of the hopping integrals, which depend on the cell volume and distortions. In the REMnO_3 series the volume decreases with ionic radius. Tilting and rotation, however, increase, because of the increasing mismatch between the Mn-O and RE-O bond-lengths. For LaMnO_3 a volume collapse at T_{OO} has been reported [15]. Under pressure, up to $P=18$ GPa the volume decreases by $\sim 10\%$, while tilting/rotation slightly decrease. A sizable

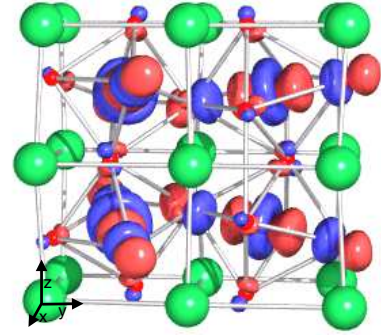


FIG. 1: (Color online) Orbital-order in TbMnO_3 , as obtained by LDA+DMFT calculations. The pseudo-cubic axes pointing along Mn-Mn bonds are shown in the left corner.

volume reduction typically increases the Mn-O hopping integrals, while tilting and rotation tends to reduce them, reducing super-exchange effects. The scenario is further complicated by the local crystal-field [6, 16, 17], which can, depending on its size and symmetry, help or compete with super-exchange, and thus even reverse the trends.

In this Letter we clarify the role of super-exchange in orbital-melting. We show that, already in the absence of crystal-field splitting, only in LaMnO_3 $T_{KK} \sim T_{OO}$, while in all other systems T_{KK} is 2-3 times smaller than T_{OO} : While T_{OO} strongly increases with decreasing IR , T_{KK} slightly decreases. Taking the tetragonal crystal-field splitting into account, these trends are enhanced even further. This proves that, although very large, in view of the reported experimental trends, super-exchange plays a minor role in the orbital-melting transition. In order to quantify the role of many-body super-exchange in determining T_{OO} , we perform ab-initio calculations based on the local density approximation (LDA) + dynamical mean-field theory (DMFT) method [18] in the paramagnetic phase. The minimal model Hamiltonian to study super-exchange effects in manganites is the Hubbard model for the e_g bands in the magnetic field

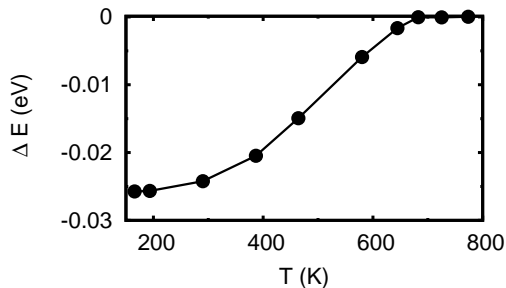


FIG. 2: Energy gain per formula unit due to orbital-ordering (LaMnO₃). Error bars are smaller than the symbols.

$h = JS_{t_{2g}}$ of disordered t_{2g} spins $\mathbf{S}_{t_{2g}}$ [19]

$$\begin{aligned}
H = & \sum_i \varepsilon_{JT} \tau_{ix} + \varepsilon_T \tau_{iz} - \sum_{i \neq i', m \sigma m' \sigma'} t_{m, m'}^{i, i'} u_{\sigma, \sigma'}^{i, i'} c_{i m \sigma}^\dagger c_{i' m' \sigma'} \\
& - h \sum_{im} (n_{im\uparrow} - n_{im\downarrow}) + U \sum_{im} n_{im\uparrow} n_{im\downarrow} \\
& + \frac{1}{2} \sum_{im(\neq m')\sigma\sigma'} (U - 2J - J\delta_{\sigma, \sigma'}) n_{im\sigma} n_{im'\sigma'}. \quad (1)
\end{aligned}$$

Here $c_{im\sigma}^\dagger$ creates an electron with spin $\sigma = \uparrow, \downarrow$ in a Wannier orbital $|m\rangle = |x^2 - y^2\rangle$ or $|3z^2 - 1\rangle$ at site i , and $n_{im\sigma} = c_{im\sigma}^\dagger c_{im\sigma}$. \uparrow (\downarrow) indicates the e_g spin parallel (antiparallel) to the t_{2g} spins (on that site). In the paramagnetic state, the matrix u ($u_{\sigma, \sigma'}^{i, i'} = 2/3$) accounts for the orientational disorder of the t_{2g} spins [19]; $t_{m, m'}^{i, i'}$ is the LDA [20] hopping integral from orbital m on site i to orbital m' on site $i' \neq i$, obtained *ab-initio* by down-folding the LDA bands and constructing a localized e_g Wannier basis. The on-site term $\varepsilon_{JT} \tau_{ix} + \varepsilon_T \tau_{iz}$ yields the LDA crystal-field matrix. It is the sum of a Jahn-Teller ($\varepsilon_{JT} \tau_{ix}$) and a tetragonal ($\varepsilon_T \tau_{iz}$) term, where τ_{ix} and τ_{iz} are the pseudospin-1/2 operators $\tau_{ix} = \frac{1}{2} \sum_{\sigma, m \neq m'} c_{im\sigma}^\dagger c_{im'\sigma}$, $\tau_{iz} = \frac{1}{2} \sum_{\sigma, m} (-1)^{\delta_{m, x^2 - y^2}} c_{im\sigma}^\dagger c_{im\sigma}$. U and J are the direct and exchange screened on-site Coulomb interaction. We use the theoretical estimates $J = 0.75$ eV, $U \sim 5$ eV [6, 21, 22] and $2JS_{t_{2g}} \sim 2.7$ eV [22]; we find that, in the high-spin regime, T_{KK} is not sensitive to the specific value of $2JS_{t_{2g}}$, therefore we keep h fixed in all results we present. We solve (1) within DMFT [23] using a quantum Monte Carlo [24] solver, working with the full self-energy matrix $\Sigma_{mm'}$ in orbital space [17]. We construct the LDA Wannier functions via the downfolding procedure based on the Nth-Order Muffin-Tin (NMTO) method [20]. Additionally, we perform LAPW calculations [25], and construct maximally localized Wannier functions [26]. The band-structures and parameter trends obtained with the two methods are very similar [27].

To determine the super-exchange transition temperature T_{KK} we use two independent approaches. In the

first, we calculate the order parameter p as a function of temperature T , in the second we determine the $T = 0$ total energy gain $\Delta E(p)$ (Fig. 2) due to orbital order.

The order parameter for orbital-ordering is the orbital polarization $p \equiv |n_1 - n_2|$, where $|1\rangle$ and $|2\rangle$ are the natural orbitals in e_g -space. To determine T_{KK} we perform LDA+DMFT calculations as a function of temperature for all materials in the series. They differ in (i) hopping integrals and (ii) crystal field, due to static distortions. In order to separate the effects of super-exchange from those of the crystal field, we perform LDA+DMFT calculations of the orbital polarization as a function of temperature for the real system (H^{LDA}), for ideal structures with the same hopping integrals but no crystal-field splitting (Fig. 3), and for ideal structures with only tetragonal splitting (Fig. 4).

In the second approach we calculate the energy gain due to orbital order from the difference in total energy between the orbitally polarized and the orbitally disordered states, in the absence of crystal fields ($\varepsilon_T = \varepsilon_{JT} = 0$). We first perform LDA+DMFT calculations for decreasing temperature and calculate the total energy per formula unit and polarization p , $E_{\text{TOT}}(p)$. Next, we repeat the same procedure, but with the constraint $p = 0$ ($\Sigma_{1,1} = \Sigma_{2,2}$ and $\Sigma_{1,2} = 0$).

The total energy is given by [28],

$$E_{\text{TOT}}(p) = E_{\text{TOT}}^{\text{LDA}} + \langle H \rangle_p - E_{e_g}^{\text{LDA}} - E_{\text{DC}},$$

where $E_{\text{TOT}}^{\text{LDA}}$ is the LDA total-energy, $E_{e_g}^{\text{LDA}}$ the thermal average of (1) in the non-interacting ($\hat{U} = 0, J = 0$) case, $\langle H \rangle_p$ the actual thermal average of (1) in DMFT for polarization p , and E_{DC} the double counting correction. Of all these terms only $\langle H \rangle_p$ contributes to

$$\Delta E(p) = E_{\text{TOT}}(p) - E_{\text{TOT}}(0) = \langle H \rangle_p - \langle H \rangle_{p=0}. \quad (2)$$

$\langle H \rangle_p$ can be split into a single-electron contribution (from the first three terms in (1)), which we calculate as sum on Matsubara frequencies, and a correlation contribution (from the last two terms in (1)), which we obtain from the double-occupancy matrix. Since $-\Delta E_{\text{TOT}}(p) \sim 10 - 50$ meV, error bars, in particular the QMC statistical error on the double-occupancies matrix, have to be controlled to high accuracy [29]. The total-energy gain for LaMnO₃ is shown in Fig. 2. We obtain similar behavior for the other systems. In the zero-temperature limit, we extrapolate from $\Delta E(p)$ the super-exchange energy gain $\Delta E_{\text{KK}} = E_{\text{TOT}}(p = 1) - E_{\text{TOT}}(p = 0)$. Remarkably, we find that the static mean-field [31] relation $T_{\text{KK}} \equiv |2\Delta E_{\text{KK}}|/k_B$, which is valid for spin-1/2 Heisenberg-like model [1] with arbitrary coupling constants, gives transition temperatures close to those obtained from order-parameter calculations, the difference being a mere small shift. Our results are shown in Fig. 3. While $T_{\text{KK}} \sim T_{\text{OO}}$ in LaMnO₃, in all other systems T_{KK} is a factor 2-3 smaller than the experimental estimate for T_{OO} . Moreover, T_{KK} is maximum in

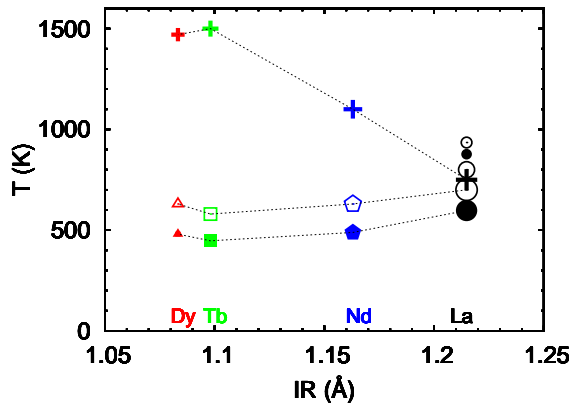


FIG. 3: (Color online) Orbital-order transition temperature T_{KK} [30] in rare-earth manganites REMnO_3 versus RE^{3+} radius, with $\text{RE}=\text{Dy}$ (triangles), Tb (squares), Nd (pentagons), La (circles). Full symbols: T_{KK} from LDA+DMFT total energy. Empty symbols: T_{KK} from LDA+DMFT order parameter calculations. Symbols of decreasing size: $P=0$ GPa, 5.4 GPa and 9.87 GPa. Crosses: Experimental values (ambient pressure) from Refs. [10–12].

LaMnO_3 , and roughly decreases with IR from $\text{RE}=\text{La}$ to Tb , then increases again. T_{KK} also increases under pressure. These trends are opposite to those reported experimentally for the orbital melting temperature. They can be ascribed to the increasing distortions along the REMnO_3 series, and the decrease in volume and tilting/rotation with increasing pressure. Finally, for all systems super-exchange favors the occupation of the orbital (signs are given for the site displayed in Fig. 4) $|\theta\rangle = -\sin\frac{\theta}{2}|x^2-y^2\rangle + \cos\frac{\theta}{2}|3z^2-1\rangle$, with $\theta = 90^\circ$, while experimentally $\theta \sim 108^\circ$ in LaMnO_3 increasing with decreasing IR to 114° in TbMnO_3 [32].

Due to the competition between the tetragonal crystal-field splitting ε_T and super-exchange (which favor the occupation of different orbitals), T_{KK} is reduced even further. We find that for finite ε_T the system is orbitally ordered already at high temperature due to the crystal field, but the occupied orbital has $\theta = 180^\circ$. In Fig. 4 we show the results for ε_T fixed at ~ 130 meV, sizable but smaller than for any of the considered systems (see Fig. 5). We find that at the reduced critical temperature $T_{\text{KK}}^{\varepsilon_T}$, super-exchange rotates the orbital towards 90° . The change in T_{KK} for LaMnO_3 , but T_{KK} is reduced to 400 K for NdMnO_3 , and even more for DyMnO_3 and TbMnO_3 . Furthermore, in the zero-temperature limit, the smaller $T_{\text{KK}}^{\varepsilon_T}$, the closer is θ to 180° . Thus a fixed $\varepsilon_T \sim 130$ meV enhances the trend found for $\varepsilon_T = 0$: T_{KK} is larger in LaMnO_3 , and decreases going to DyMnO_3 . Still, even for LaMnO_3 , θ is significantly larger than the experimental 108° . This means that a Jahn-Teller crystal-field splitting ε_{JT} is necessary to explain the experimental θ ; Fig. 4 shows that

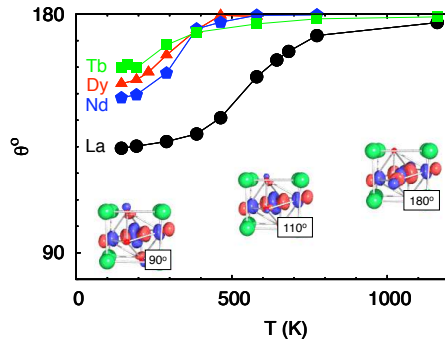


FIG. 4: (Color online) Rotation of the occupied state $|\theta\rangle$ as a function of temperature in the presence of a 130 meV tetragonal crystal field. The orbitals are shown for TbMnO_3 .

such splitting has to increase for the series $\text{RE}=\text{La}$, Nd , Dy , Tb . Taking into account that tetragonal splitting actually increases with decreasing pressure, and substituting La with Nd , Tb , or Dy (Fig. 5), this trend is enhanced even more. For ε_T corresponding to the real structures, down to 150 K we find no super-exchange transition for all systems but LaMnO_3 . These results can be understood qualitatively in static mean-field theory. In this approach, super-exchange yields an effective Jahn-Teller splitting $\varepsilon_{\text{KK}} = \langle \tau_x \rangle \lambda_{\text{KK}}$, where λ_{KK} is the molecular field parameter; the self-consistency condition for orbital order is $\langle \tau_x \rangle = \frac{1}{2} \sin\theta \tanh\left(\beta\sqrt{\varepsilon_T^2 + \varepsilon_{\text{KK}}^2}/2\right)$, with $\sin\theta = \varepsilon_{\text{KK}}/\sqrt{\varepsilon_T^2 + \varepsilon_{\text{KK}}^2}$. This equation has a non-trivial solution ($\theta \neq 180^\circ$) only if $\lambda_{\text{KK}}/2 > \varepsilon_T$. The critical temperature is $T_{\text{KK}}^{\varepsilon_T}/T_{\text{KK}}^0 = (\varepsilon_T/2k_B T_{\text{KK}}^0)/\tanh^{-1}(\varepsilon_T/2k_B T_{\text{KK}}^0)$, with $k_B T_{\text{KK}}^0 = \lambda_{\text{KK}}/4$; it decreases with increasing ε_T , while $\theta \rightarrow 180^\circ$ [33]. For large enough ε_T ($\varepsilon_T > \lambda_{\text{KK}}/2$) there is no super-exchange driven transition at all.

In conclusion, for the orbital-melting transition in rare-earth manganites REMnO_3 , we find that many-body super-exchange yields a transition temperature T_{KK} very close to T_{OO} only in LaMnO_3 , while in all other systems T_{KK} is less than half T_{OO} . Moreover, we find that super-exchange yields $\theta \sim 90^\circ$ for the occupied orbital, while in the experimental structures $\theta \sim 108^\circ - 114^\circ$. We also find that a tetragonal splitting ε_T reduces T_{KK} even further. ε_T increases substituting La with Nd , Tb or Dy and decreases under pressure. Finally, super-exchange effects become larger with increasing pressure, while experimentally orbital order eventually melts [13, 14]. Our work proves that, in the light of the experimentally observed trends, super-exchange plays a minor role in the orbital-melting transitions of rare-earth manganites.

We thank I. Loa and K. Syassen for sharing unpublished data. Calculations were done on the Jülich Blue Gene/P. We acknowledge financial support from the

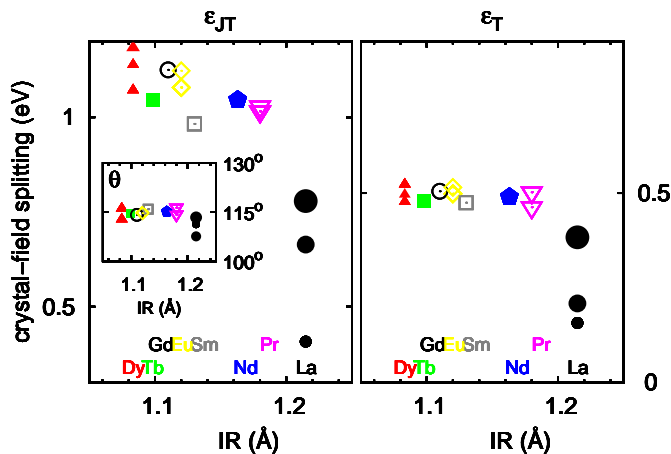


FIG. 5: (Color online) Evolution of the crystal-field (Jahn-Teller and tetragonal) as a function of the rare-earth ion radius calculated for all structures reported in Refs. [11, 34–36]. Filled circles of decreasing size: LaMnO₃ for P=0, 5.4 and 9.87 GPa [13]. Inset: calculated occupied orbital.

Deutsche Forschungsgemeinschaft through research unit FOR1346.

* Electronic address: e.pavarini@fz-juelich.de

[1] K.I. Kugel and D.I. Khomskii, Zh. Eksp. Teor. Fiz. **64**, 1429 (1973) [Sov. Phys. JEPT **37**, 725 (1973)].
 [2] J.B. Goodenough, Phys. Rev. **100**, 564 (1955); J. Kanamori, J. Appl. Phys. Supp. **31**, 148 (1960).
 [3] Y. Tokura and N. Nagaosa, Science **288**, 462 (2000); S.-W. Cheong, Nature Materials **6**, 927 (2007); E. Dagotto and Y. Tokura, MRS Bull. **33**, 1037 (2008); M. Imada, A. Fujimori, and Y. Tokura, Rev. Mod. Phys. **70**, 1039 (1998)
 [4] W.-G. Yin, D. Volja, and W. Ku, Phys. Rev. Lett. **96**, 116405 (2006).
 [5] D. Feinberg, P. Germain, M. Grilli, and G. Seibold, Phys. Rev. B **57**, R5583 (1998); C. Lin and A. J. Millis, Phys. Rev. B **78**, 174419 (2008).
 [6] E. Pavarini, E. Koch, A.I. Lichtenstein, Phys. Rev. Lett. **101**, 266405 (2008); E. Pavarini and E. Koch, Phys. Rev. Lett. **104**, 086402 (2010).
 [7] M.C. Sánchez, G. Subías, J. García, and J. Blasco, Phys. Rev. Lett. **90**, 045503 (2003); X. Qiu, Th. Profen, J.F. Mitchell, and S.J.L. Billinge, *ibid.* **94**, 177203 (2005); A. Sartbaeva *et al.*, *ibid.* **99**, 155503 (2007).
 [8] A. Y. Ramos *et al.*, Phys. Rev. B **75**, 052103 (2007); M. Baldini *et al.*, Phys. Rev. Lett. **106**, 066402 (2011).
 [9] J. Rodríguez-Carvajal *et al.*, Phys. Rev. B **57**, R3189 (1998); Y. Murakami *et al.*, Phys. Rev. Lett. **81**, 582 (1998).
 [10] J.-S.Zhou and J. B. Goodenough, Phys. Rev. B **68**, 144406 (2003); J.-S.Zhou and J. B. Goodenough, Phys. Rev. Lett. **96**, 247202 (2006).
 [11] B. Dabrowski *et al.*, J. Solid State Chem. **178**, 629 (2005).
 [12] G. Maris, V. Volotchaev, and T.T.M. Palstra,

New. J. Phys. **6**, 153 (2004).
 [13] I. Loa *et al.*, Phys. Rev. Lett. **87**, 125501 (2001); I. Loa and K. Syassen, private communication.
 [14] J. M. Chen *et al.*, Phys. Rev. B **79**, 165110 (2009).
 [15] T. Maitra, P. Thalmeier, and T. Chatterji, Phys. Rev. B **69**, 132417 (2004).
 [16] E. Gorelov *et al.*, Phys. Rev. Lett. **104**, 226401 (2010).
 [17] E. Pavarini *et al.*, Phys. Rev. Lett. **92**, 176403 (2004).
 [18] V. Anisimov *et al.*, J. Phys.: Condens. Matter **9**, 7359 (1997); A. I. Lichtenstein and M. I. Katsnelson, Phys. Rev. B **57** 6884 (1998).
 [19] K.H. Ahn, A.J. Millis, Phys. Rev. B **61**, 13545 (2000). In the high-spin regime the orbital superexchange coupling depends weakly on $u_{\sigma,-\sigma}$ terms [6]; thus we neglect them.
 [20] See E. Pavarini, A. Yamasaki, J. Nuss and O. K. Andersen, New J. Phys. **7**, 188 (2005).
 [21] T. Mizokawa and A. Fujimori, Phys. Rev. B **54**, 5368 (1996).
 [22] A. Yamasaki *et al.*, Phys. Rev. Lett. **96**, 166401 (2006).
 [23] A. Georges, G. Kotliar, W. Kraut, M. J. Rozenberg, Rev. Mod. Phys. **68**, 13 (1996).
 [24] J. E. Hirsch and R. M. Fye, Phys. Rev. Lett. **56**, 2521 (1986).
 [25] P. Blaha, K. Schwarz, G. Madsen, D. Kvasnicka and J. Luitz, WIEN2k, *An Augmented Plane Wave + Local Orbitals Program for Calculating Crystal Properties* (Karlheinz Schwarz, Techn. Universität Wien, Austria), 2001. ISBN 3-9501031-1-2.
 [26] A. A. Mostofi *et al.*, Comp. Phys. Comm. **178**, 685 (2008); J. Kunes *et al.*, *ibid.* **181**, 1888 (2010).
 [27] LaMnO₃: $\epsilon_T \sim 350$ meV, $\epsilon_{JT} = 650$ meV, $t_{3z^2-1,3z^2-1}^{001} = 392$ meV. TbMnO₃: $\epsilon_T \sim 580$ meV, $\epsilon_{JT} = 1060$ meV, $t_{3z^2-1,3z^2-1}^{001} = 349$ meV. See Fig. 5 for comparison with NMO results.
 [28] A. K. McMahan, K. Held, and R. T. Scalettar, Phys. Rev. B **67**, 075108 (2003); B. Amadon, S. Biermann, A. Georges, and F. Aryasetiawan, Phys. Rev. Lett. **96**, 066402 (2006); I. Leonov *et al.*, Phys. Rev. Lett. **101**, 096405 (2008).
 [29] A simple estimate from the average correlation energy, $\frac{1}{2}U n_{e_g}(n_{e_g}-1)$, is $\frac{1}{2}(U(2n_{e_g}-1))\delta n_{e_g} \ll |\Delta E(p)|$, which for $\Delta E(p) \sim -10$ meV, $n_{e_g} = 1$ and $U = 5$ eV, yields $\delta n_{e_g} \ll 4 \cdot 10^{-3}$.
 [30] All results shown are for $U = 5$ eV and $J = 0.75$ eV. For $P = 9.87$ GPa, setting $\epsilon_T = \epsilon_{JT} = 0$ we obtain however a metallic solution with $p = 0$. Since T_{KK} decreases with U roughly as $\sim 1/U$, as expected from super-exchange theory, to compare values for constant U , we then extrapolate the $U = 5$ eV value of T_{KK} from the insulating state obtained for slightly larger U ($U = 5.5$ eV, $U = 6$ eV).
 [31] W. Nolting and A. Ramakanth, *Quantum theory of Magnetism*, Springer (2009), p. 306.
 [32] M.W. Kim *et al.*, Phys. Rev. Lett. **96**, 247205 (2006).
 [33] The energy gain due to the pseudospin rotation is $2|\Delta E|/k_B T_{KK}^{\epsilon_T} = (1-x)^2(\tanh^{-1}x)/x$, where $x = 2\epsilon_T/\lambda_{KK}$. For $\theta = 130^\circ$ (as for LaMnO₃, Fig. 4) we find $T_{KK}^{\epsilon_T} \sim 0.84T_{KK}^0$ and $2|\Delta E|/k_B T_{KK}^{\epsilon_T} \sim 0.15$. This ratio is in qualitative agreement with what we find with DMFT for LaMnO₃, $|\Delta E| \sim 10$ meV.
 [34] J. A. Alonso *et al.*, Inorg. Chem. **39**, 917 (2000).
 [35] T. Mori *et al.*, Mat. Lett. **54**, 238 (2002).
 [36] K. Uusi-Esko *et al.*, Mater. Chem. Phys. **112**, 1029 (2008).